

Received: 2016.01.08
Accepted: 2016.03.16
Published: 2016.05.30

The First Reported Case of Erdheim-Chester Disease in Egypt with Bilateral Exophthalmos, Loss of Vision, and Multi-Organ Involvement in a Young Woman

Authors' Contribution:

Study Design A
Data Collection B
Statistical Analysis C
Data Interpretation D
Manuscript Preparation E
Literature Search F
Funds Collection G

CDE 1 **Emad E. Abdellateef**
ABCDEFG 1 **Ayman R. Abdelhai**
ABCG 2 **Heba H. Gawish**
BDF 3 **Ghada A. Abdulmonaem**
D 4 **Eman H. Abdelbary**
B 1 **Ahmed I. Ahmed**

1 Department of Internal Medicine, Zagazig University, Faculty of Medicine, Zagazig, Egypt
2 Department of Clinical Pathology, Zagazig University, Faculty of Medicine, Zagazig, Egypt
3 Department of Radiology, Zagazig University, Faculty of Medicine, Zagazig, Egypt
4 Department of Pathology, Zagazig University, Faculty of Medicine, Zagazig, Egypt

Corresponding Author: Ayman R. Abdelhai, e-mail: Aymedman@yahoo.co.uk
Conflict of interest: None declared

Patient: Female, 19
Final Diagnosis: Erdheim-Chester disease
Symptoms: Exophthalmos, orthopnea
Medication: Prednisolone • azathioprine
Clinical Procedure: —
Specialty: Internal Medicine

Objective: Unknown etiology

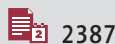
Background: Erdheim-Chester disease is a rare non-Langerhans-cell histiocytosis of unknown etiology with multi-organ involvement.

Case Report: A 19-year-old woman presented with orthopnea, severe fatigue, bilateral exophthalmos, and gradual loss of vision. She had anemia and mild leucocytosis related to chronic illness. Marked left side pleural effusion and massive pericardial effusion with bilateral hydronephrosis were detected by plain X-ray, echocardiography, and computed tomography, respectively. Retro-orbital tissue and bone marrow biopsy revealed histiocytic infiltration, which was CD68-positive and CD1a-negative.

Conclusions: This report describes the first case presentation of Erdheim-Chester disease in our country. This case report may advance our understanding of an orphan disease. Our patient's young age and stable clinical status may allow long-term follow-up of treatment results.

MeSH Keywords: Bone Marrow • Cardiac Tamponade • Exophthalmos • Histiocytosis, Non-Langerhans-Cell

Full-text PDF: <http://www.amjcaserep.com/abstract/index/idArt/897479>



2387



1



7



29



Background

Erdheim-Chester disease (ECD) is a rare disorder that was first described by Jakob Erdheim and William Chester in 1930 [1]. There have been up to 600 cases reported to date, primarily males ages 50–70 years old [2]. According to the WHO classification, ECD is a neoplasm deriving from histiocytes, but there is a long-standing debate as to whether the disorder is of malignant or polyclonal reactive nature [3]. Clinical manifestations of ECD at presentation are protean and encompass bone pain, diabetes insipidus, and neurological and constitutional symptoms, although retroperitoneal, cutaneous, cardiovascular, and pulmonary involvement have also been described [4,5].

Systemic manifestations of ECD are peculiar and their radiological appearance make the diagnosis rather easy. The symmetric bilateral osteosclerosis of the metaphysis and diaphysis of long bones (74%); the sheathing of the whole thoraco-abdominal aorta, called “coated aorta” (16%); and the perirenal fascia infiltration taking the appearance of “hairy kidneys” (6%) are highly suggestive features of the disease [6]. Histopathological and immunohistochemical examination is mandatory for definite diagnosis and to differentiate ECD from other types of histiocytosis [7]. To the best of our knowledge, this is the first published case of ECD described in Egypt. Herein, we report on a unique case of ECD presented by undiagnosed bilateral exophthalmos with loss of vision for years in a young woman.

Case Report

In April 2009, a 13-year-old girl with no significant medical history was referred to an ophthalmologist with unilateral left exophthalmos. Physical examination of the patient at that time was normal except for unilateral exophthalmos. White blood cell, hemoglobin, and platelet counts were 3.180 cell/mm³, 10.5 g/dL, and 6376.000/mm³, respectively. There was no albumin/globulin ratio reversal. Serum blood urea nitrogen and creatinine levels were 18 and 0.6 mg/dL, respectively. There was no proteinuria. Thyroid-stimulating hormone and free thyroxine levels were 2.63 µIU/mL and 1.71 ng/mL, respectively. Chest radiograph was normal. Normal-sized kidneys and normal liver and spleen span were observed by abdominal ultrasonography.

The patient was lost to follow-up until January 2015, when she began to visit the ophthalmology clinic because of marked bilateral exophthalmos and gradual loss of vision. The patient's complete blood count was compatible with anemia of chronic disease accompanied by mild thrombocytosis (550.000/mm³). Decompression surgery was done to alleviate the tissue pressure over the optic nerve, with no improvement of vision. Histopathological examination of the removed orbital tissue showed the presence of xanthogranulomatous tissue. No

further surgical treatment was attempted at that time. The patient was treated with a short course of steroids, which resulted in no improvement of the exophthalmos or the vision acuity. The patient was discharged from the ophthalmology unit without definite diagnosis or plans for medical therapy or follow-up.

In October 2015, the patient presented with orthopnea and bilateral mild lower-limb edema to our Internal Medicine Department of Zagazig University Hospital. On physical examination, she had bilateral +1 lower-limb edema, bilateral severe exophthalmos, and left side yellowish plaque (xanthoma) on the left upper eyelid. Her visual acuity was counting fingers in the left eye and blind right eye. There was irregular asymmetric thyroid enlargement, stony dullness up to the 5th rib from the back on the left side with diminished air entry, distant heart sounds, pallor, and fever (38.5°C). The rest of the clinical examination was unremarkable (Figure 1).

Laboratory tests showed leukocytosis, anemia, and thrombocytosis. Renal and liver function tests and lipid profile were normal. White blood cell, hemoglobin, and platelet counts were 18.190 cell/mm³, 7.2 g/dL, and 660.000/mm³, respectively. Serum blood urea nitrogen and serum creatinine levels were 22 mg/dL and 1.4 mg/dL, respectively. There was no albumin/globulin ratio reversal. Urine test for Bence-Jones protein was negative. ANA and anti-dsDNA were negative. All laboratory results of our patient are shown in Table 1.

Radiological and imaging findings

Chest radiography showed cardiomegaly and an urgent echocardiography showed a large pericardial effusion with echocardiographic features of cardiac tamponade. Figure 2 shows the images before and after drainage.

Multi-slice CT axial cuts of the chest after an intravenous contrast study revealed moderate to severe pericardial effusion and the thoracic aorta showed minimal periaortic infiltration, mainly frontal aspect of its arch with moderate left side pleural effusion, which exerted left lower lobe collapse. There were no significant focal lesions or infiltrations in the lung parenchyma (Figure 3). Transthoracic echocardiography revealed a large pericardial effusion with abnormal right heart filling. Left ventricular ejection fraction was slightly reduced. The patient was subjected to diagnostic and therapeutic pericardiocentesis and thoracocentesis with drainage of about 1200 mL and 2000 mL of serous fluid, respectively. Results of microbiological and cytological examinations on pericardial fluid were negative (Table 1). Pleural and pericardial drains were left for 1 week until depletion of the fluid drained.

Conventional plain radiography of both lower limbs showed more or less bilateral symmetric progressing osteosclerotic



Figure 1. (A) frontal and (B) lateral views of our patient showed bilateral severe exophthalmos, xanthoma on the left upper eyelid (C).

changes predominantly at metaphysis and diaphysis of both femora and heterogeneous osteosclerosis of the cancellous bone was clearly depicted at the proximal tibia at both sides with relative narrow marrow cavity (Figure 4A, 4B). The patient underwent axial and reformatted coronal CT of the femora, which helped confirm cortical thickening and showed heterogeneous sclerosis of the cancellous bone (Figure 4C, 4D). Technetium-99m bone scintigraphy showed areas of increased tracer uptake described as symmetric activity elevation by both iliac bones and distal tibiae (Figure 4E) sparing the epiphysis but more exuberant in posterior parts of both ileae.

Multi-slice pre- and post-contrast CT imaging of the orbits revealed a hyperdense lesion diffusely involving the orbit (Figure 5A). Magnetic resonance imaging disclosed diffuse

infiltration of the orbits, with a hypointense lesion in T1 images (Figure 5B, 5C).

The CT and MRI of the abdomen showed mild bilateral hydronephrosis with the presence of perirenal infiltration, which gives the appearance of “hairy kidney” on the left side and minimal amount of free intra-peritoneal fluid, associated with enlarged adrenal glands at both sides; the rest of the examination was unremarkable (Figure 6A–6D).

During the hospitalization a surgical intervention was performed and a retro-orbital tissue sample was collected from the right eye and left eye as decompression maneuver and biopsy sample. Samples were fixed in 10% buffered formalin, embedded in paraffin, and stained with hematoxylin and

Table 1. The laboratory results of our patient during the period of her hospital admission.

Item	Results by date		
	04-10-2015	17-10-2015	27-10-2015
WBC ($\times 10^3/\mu\text{L}$)	11.4	27.1	21
Neutrophils ($\times 10^3/\mu\text{L}$)	7.2	19.9	13.6
Hemoglobin (gm/dl)	7.3	11.8	11.9
Platelets ($\times 10^3/\mu\text{L}$)	622	573	491
Absolute reticulocytic count ($\times 10^6/\mu\text{L}$)	151800		
Direct Coombs test	Negative		
ESR (mm)	55/100 (1 st /2 nd hour)		
Serum total proteins (g/dl)	5.6	6	5.8
Serum albumin (g/dl)	3.03	2.85	2.9
Serum creatinine(g/dl)	1.3	1	0.9
Serum urea (g/dl)	15	17	16
Serum iron ($\mu\text{g/dl}$)	9.2 (Normal=60–160)		
Total iron binding capacity ($\mu\text{g/dl}$)	153.3 (Reference range=255–450)		
Unsaturated iron binding capacity ($\mu\text{g/dl}$)	144.1 (Reference range=135–392)		
Serum ferritin (ng/ml)	121 (Reference range=13–150)		
INR	1.11		
ANA	Negative		
Anti-ds.DNA	Negative		
Serum uric acid (mg/dl)	7.2	6	
Serum Na (mmol/L)	143		
Serum K (mmol/L)	3.6		
Serum Ca(mg/dL)	8	9	
Serum P (mg/dl)	3.75	4	
Total protein in 24-h urine (mg/24 hour)	218.4		
TSH (mIU/ml)	2.2 (Reference range=0.3–4.2)	1.7	
Free T4 (pmol/L)	20.8 (Reference range=12–22)	15	
Serum LDH (U/L)	293 (Reference range=240–480)	265	
Serum cholesterol (mg/dl)	266	230	
Serum triglycerides (mg/dl)	188	170	
Serum LDL (mg/dl)	160	145	
Serum HDL (mg/dl)	68	60	
Pleural fluid analysis			
Glucose (mg/dl)	79.2		
Proteins (g/dl)	3.4		
LDH (IU/L)	898		

Table 1. The laboratory results of our patient during the period of her hospital admission.

Item	Results by date		
	04-10-2015	17-10-2015	27-10-2015
Pericardial fluid analysis			
Glucose (mg/dl)	54		
Proteins (g/dl)	3.1		
LDH (IU/L)	2254		
Total leukocytic count in pleural fluid (cell/ml)	300 (normal=up to 400)		
Pleural fluid culture (aerobic and anaerobic)	Negative		
Pleural fluid cytology	No evidence of dysplastic or malignant cells		
PCR for tuberculosis (from pleural fluid)	Negative		

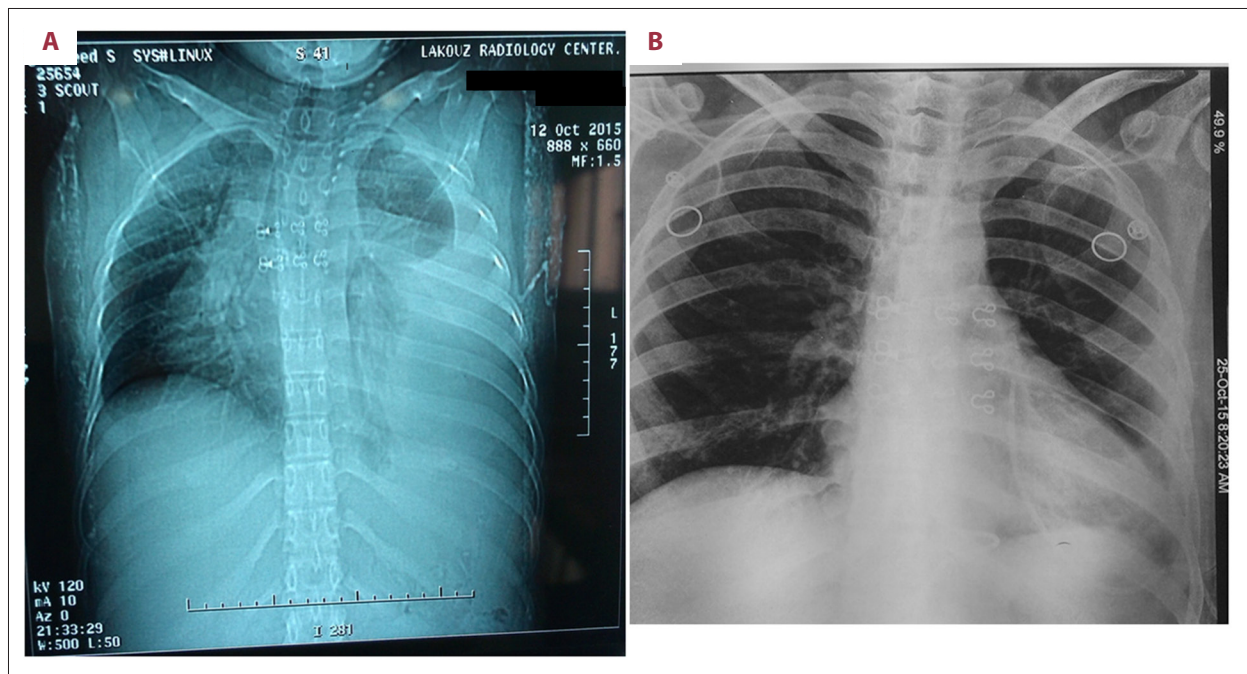


Figure 2. (A) Chest radiograph taken in the Emergency Department showed a large cardiac shadow without any significant lung pathology. (A) Before aspiration and (B) after pleural and pericardial aspiration with intercostal and pericardial drain still *in situ*.

eosin. Histopathological examination revealed dense infiltration by groups of foamy histocytes with granulomatous inflammation and focal fibrosis. There was no evidence of malignancy or specific infection (Figure 7A–7C). Immunohistochemical staining using streptavidin-biotin immunoperoxidase technique showed that these macrophages were CD68-positive but CD1a-negative (Figure 7D, 7E). Lipid vacuoles were scarce and were not suggestive of a lipid storage disease. Bone marrow biopsy was also performed, which showed hypocellular bone marrow with fatty infiltration (Figure 7F).

We made a diagnosis of ECD with involvement of the orbits, kidney, bone, bone marrow, and pleuro-pericardium based on the radiological and histopathological findings and because of dyspnea, the pleural and pericardial fluid drained, and treatment with prednisolone (30 mg/day) and azathioprine (100 mg/day) with good control after 1 month without recurrence of effusion. Echocardiography and chest X-ray 2 months after the start of treatment showed no recurrence of pericardial or pleural effusion, and the patient’s clinical condition has remained good.

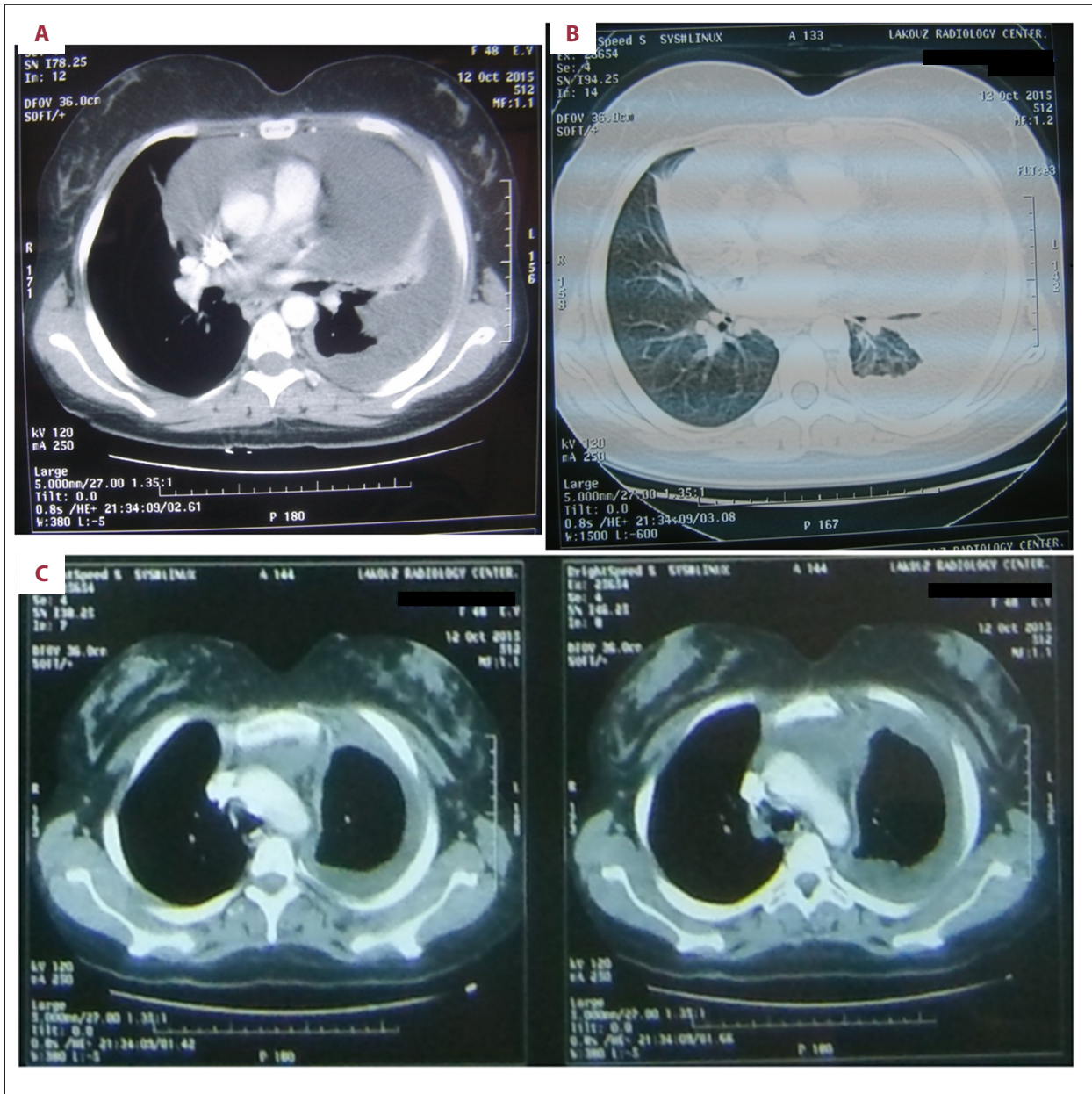


Figure 3. (A, B) Mediastinal lung windows of axial chest CT scan showed left side pleural effusion and pericardial effusion without parenchymal abnormality. (C) Axial enhanced CT image of the thoracic aorta showed minimal periaortic infiltration involving the aortic arch.

Discussion

ECD is a rare disease with very heterogeneous manifestations, from an asymptomatic and limited organ involvement to a massive and life-threatening disease. Because of its systemic presentation, ECD can be associated with general and unspecific symptoms such as weakness, fever, weight loss, sweats, and multi-organ involvement. Skeletal involvement is present in up to 96% of the patients, with symmetrical and bilateral osteosclerosis of metaphysis and diaphysis of long

bones. More than 50% of patients have at least 1 extra-skeletal manifestation, such as exophthalmos, xanthelasma, interstitial lung disease, retroperitoneal fibrosis, renal failure, diabetes insipidus, central nervous system, or cardiovascular involvement [3,8]. Radiological features are often typical, but histological examination is required for definitive diagnosis with evidence of CD68+ but CD1a- foamy histiocytes with fibrosis. CD68 is a specific histiocyte marker and CD1a is a marker for Langerhans cells; this finding distinguishes ECD from Langerhans cell histiocytosis [9].



Figure 4. (A, B) Plain radiography of both femurs and legs; (C, D) axial and coronal reformatted CT of both knees. (E) Technetium-99m bone scintigraphy showed symmetrical increased uptakes in both iliac bones and distal tibiae.

The onset of ECD is usually at 40–70 years of age, with male predominance [10]; however, our patient was a young female with disease onset at around 10 years of age. Heart involvement is more common in older patients (mean age 60 years) and no heart and/or pleuro-pericardial involvement has been

described in younger patients [6]; however, the chief complaint at the most recent presentation of our patient was exertional dyspnea due to large pleural and pericardial effusion. Death is due to cardiovascular involvement in more than one-third of cases; therefore, physicians should always look for it

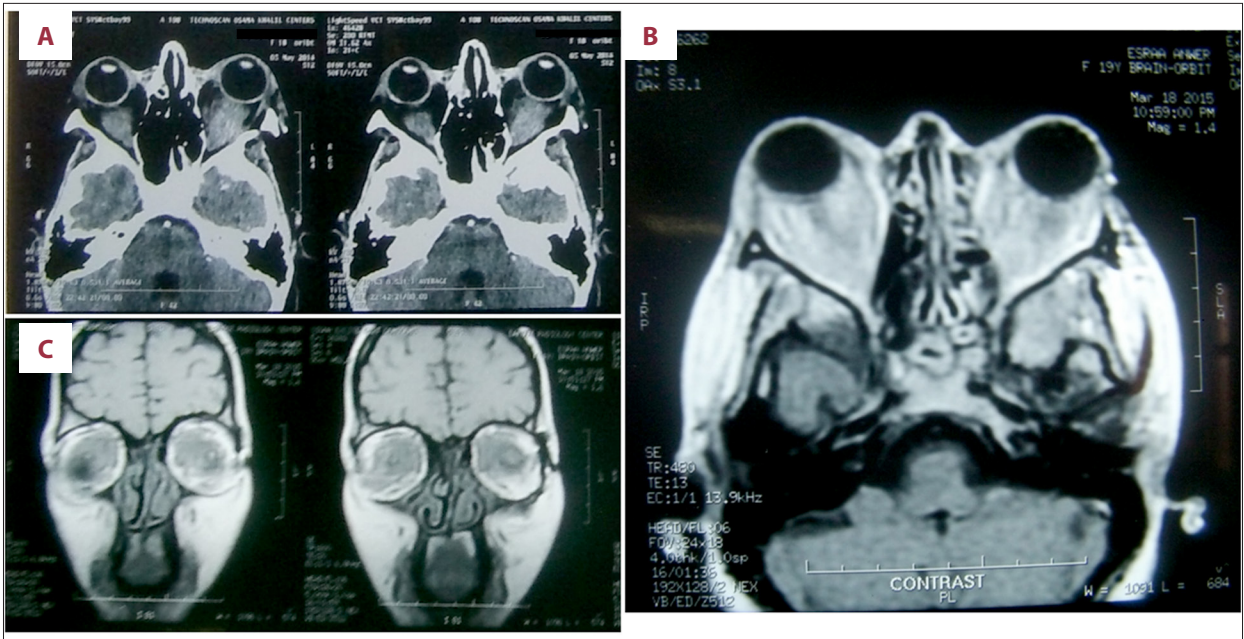


Figure 5. (A) CECT scan of both orbits showed bilateral infiltrations in and around both optic nerves and bilateral exophthalmos. (B, C) Enhanced axial and coronal T1-weighted demonstrating bilateral low-signal intensity lesions in the intraconal and extraconal spaces, and anterior to the orbital septum with significant heterogenous enhancement after contrast administration.

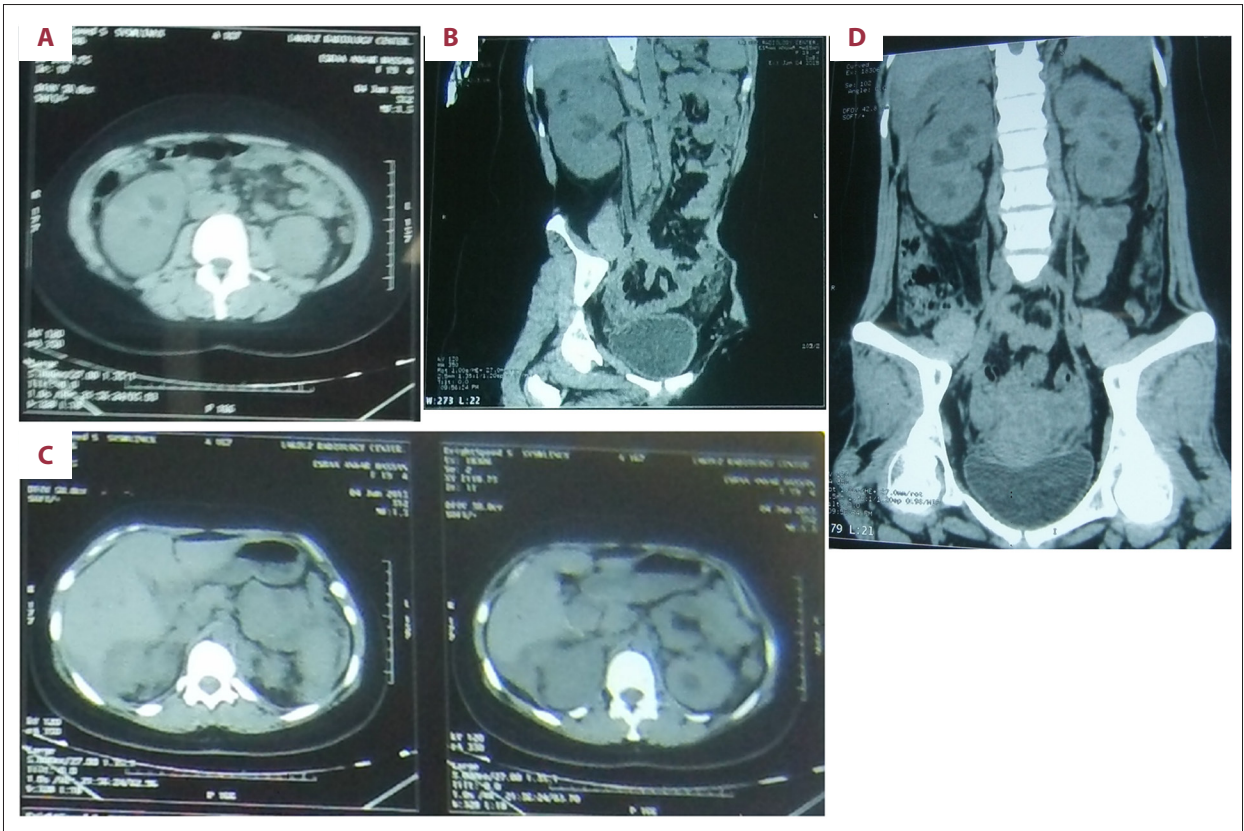


Figure 6. (A, B) Axial and reformatted coronal NECT cuts in the same patient showing bilateral and symmetric early perirenal infiltration (arrow), which gives the appearance of “hairy kidney”. (C) Axial CT scan of bilateral adrenal thickening. (D) Reformatted NECT scan shows bilateral and symmetric infiltration of the renal sinuses, with mild hydronephrosis.

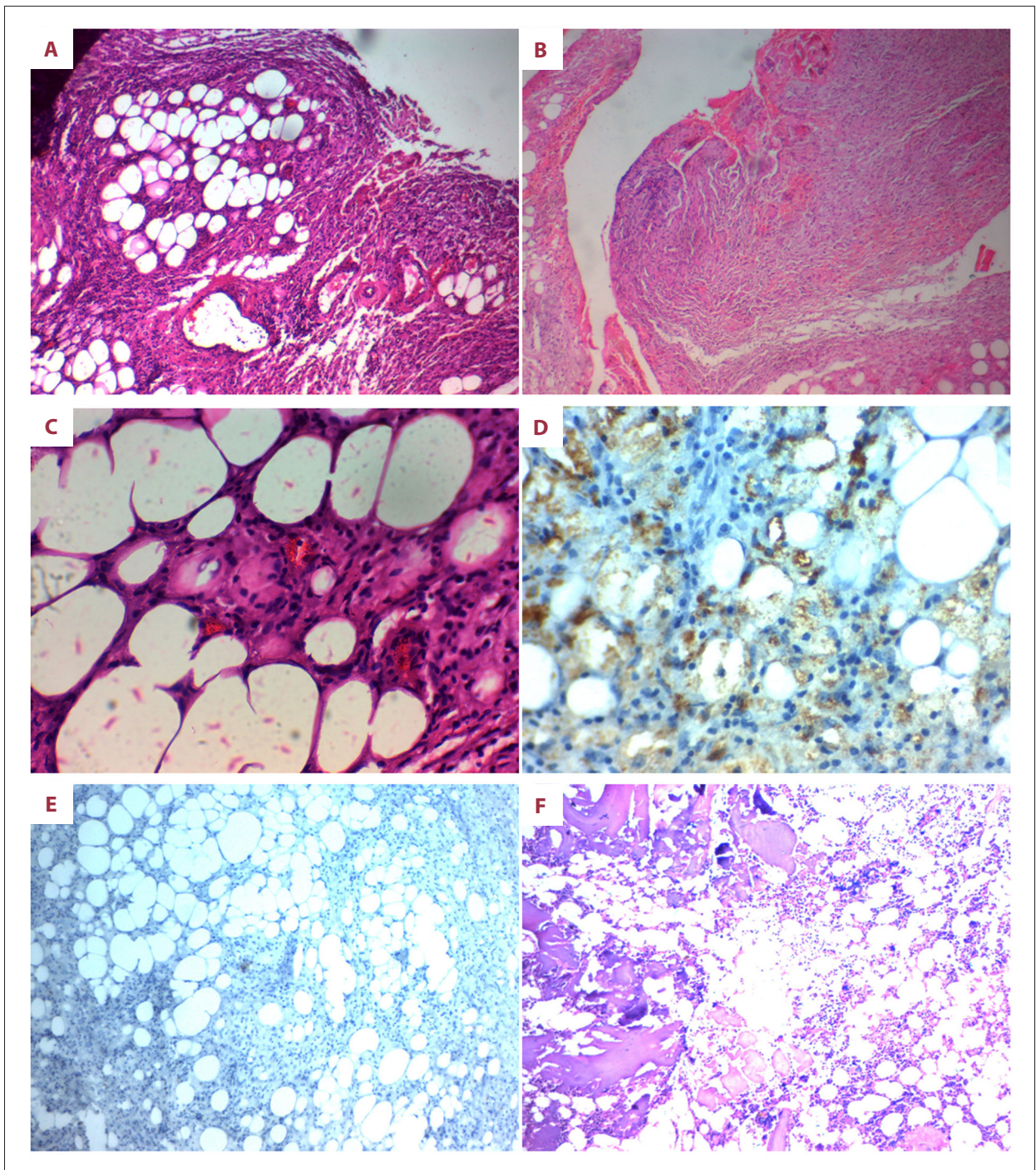


Figure 7. (A, B) Retro-orbital tissue showing infiltration of numerous foamy histiocytes (H and E; $\times 100$). (C) At higher magnification, orbital tissue is infiltrated by histiocytes with abundant eosinophilic cytoplasm (H and E; $\times 400$). (D) Retro-orbital tissue showing an infiltrate of numerous CD68-positive histiocytes (anti-CD68 Ab; $\times 400$). (E) Retro-orbital tissue showing an infiltrate of numerous CD1a-negative histiocytes (anti-CD1a Ab; $\times 100$). (F) The bone marrow biopsy showing hypocellular marrow with depression of all 3 hematopoietic elements, with foamy cells infiltration (H and E staining; $\times 100$).

when a new case of ECD is diagnosed [11,12]. The most common cardiovascular manifestation in ECD is the presence of soft tissue rounding the thoracic and abdominal aorta and its

branches, also known as “coated aorta”. The most frequent feature in heart involvement is pericardial infiltration, which may lead to cardiac tamponade [13,14].

Myocardial localized or diffuse infiltration is often observed with frequent pseudotumoral infiltration of the right atrium and involvement of the auriculoventricular sulcus [15,16]. Moreover, coronary disease with myocardial infarction, valvular dysfunction, and heart failure has been described in the literature [17]. The high frequency of pleural involvement [18] in ECD is due to lymphangitic distribution of histiocytic infiltrates, so they are mainly seen in the visceral pleura, in interlobular septa, and around the bronchovascular bundles [19]. Pulmonary radiologic features observed in ECD in the literature include smooth interlobular septal thickening, thickening of interlobar fissures, micronodules, ground-glass opacities, and parenchymal condensation. Both lungs of our patient showed no involvement and were clear on high-resolution computed tomography (HRCT) at presentation and 1 month after stabilization. Arnaud et al. [20] proposed that the diagnosis of pulmonary ECD should be considered “probable” in patients with known ECD who have findings of interstitial lung disease on HRCT scans, excluding other possible diagnoses. Pulmonary involvement in these patients can be confirmed if bronchoalveolar lavage (BAL) fluid is positive for foamy histiocytes.

Our patient complained of progressive exophthalmos over about 6 years. This presentation is common in the ECD literature. About 25% to 50% of patients have central nervous system (CNS) involvement [21], which is a leading cause of functional disability and has been found in 1 series to be an independent predictor of death [22]. Histiocytic infiltrates of the intra-axial and extra-axial compartments can occur throughout the neuraxis. They can appear similar to meningiomas or granulomatous diseases [23], which is one of the causes of delayed diagnosis in this young woman before she became our patient. Patients can present with generalized deterioration of cognition and gait disturbance if the disease is diffuse and bulky. About 25% of patients present with exophthalmos, retro-orbital pain, oculomotor palsies, or blindness due to unilateral or bilateral infiltration of the orbits. The differential diagnosis of these pseudotumoral lesions includes Graves' disease, granulomatous disease, lymphoma, and giant cell arteritis [24]. This last scenario was the first presentation of our patient, as it began by unilateral exophthalmos 6 years earlier, then progressed to bilateral exophthalmos with diminished visual acuity, which progressed to complete blindness of the right eye.

One-third of ECD patients have xanthelasma, occurring as yellow eyelid plaques, as in our case. Other sites of xanthogranulomatous involvement are the face, neck, axilla, trunk, and groin, and may appear as yellow or red-brown papules that merge into plaques. It is impossible to distinguish between xanthogranulomatous lesion of ECD and adult juvenile xanthogranulomatous (JXG) disease on the basis of skin lesions alone, but unlike ECD, JXG is less commonly a multi-system disease [10].

The typical diffuse skeletal involvement with symmetric sclerosis of the long bones is a distinct pattern of bone involvement of Erdheim-Chester disease [25]. Therefore, we evaluated skeletal involvement in our patient. Plain radiography of both tibias showed mild diffuse osteosclerotic changes. In some patients with ECD, plain films may be not conclusive; therefore, technetium-99m bone scintigraphy, which can explore the whole skeleton, is mandatory and very valuable in this situation. The axial skeleton is usually spared in cases of ECD but iliac bone involvement has been reported before [18], as in our patient. This was confirmed by the bone marrow biopsy taken from iliac bone, which revealed hypocellular marrow with infiltration by fatty cells (histiocytes). Thus, bone scintigraphy may be beneficial for early detection of skeletal involvement of ECD [26] and this role is more important in the case of unobvious changes in plain radiography, as shown in this patient.

Retroperitoneal involvement is described in more than one-third of patients with ECD and is often asymptomatic. Of note, the frequency of pseudo “retroperitoneal fibrosis” was significantly higher in male patients. Kidney infiltration or renal obstructive impairment with consequent hydronephrosis, as in our case, was described in 6% of the overall population and is often associated with the presence of retroperitoneal lesions and the X-ray appearance of “hairy kidneys”. This finding, due to the perirenal fat infiltration, appears as an irregular renal border that is emphasized by iodinated contrast and is useful for differential diagnosis with idiopathic or secondary retroperitoneal fibrosis [6].

Because of the rarity of the condition and the paucity of clinical trials, there is no definite treatment for ECD. Indeed, we have now treated our patient with systemic steroids and azathioprine for 2 months with good stabilization and no recurrence of pleural and pericardial effusion and slight improvement of visual acuity in the left eye. Although the clinical symptoms of our patient seem to be stable, there have been few reports of the efficacy of these regimens [27,28]. Therefore, close long-term follow-up will be required to evaluate the efficacy of these treatments in our patient, and searching for another effective therapy is mandatory. A promising dual therapy with anakinra, an interleukin-1-receptor antagonist, and vemurafenib, the BRAF V600 kinase inhibitor, was associated with a sustained abatement in symptoms for months [29].

Conclusions

We presented the case of an ECD patient with multi-organ involvement, diagnosed after the passage of more than 6 years from the onset of disease. This report emphasizes the need for a high index of suspicion in this diagnosis. We hope to be able to perform long-term follow-up to accurately evaluate treatment efficacy and prognosis.

Statements

This study was not conducted with research intervention, so Ethics Committee approval was not necessary.

The authors have no funding or conflicts of interest to disclose.

References:

1. Chester W: Uberlipoidgranulomatose. *Virchows Arch Pathol Anat Physiol Klin Med*, 1930; 279: 561–602 [in German]
2. Haroche J, Arnaud L, Cohen-Aubart F et al: Erdheim-Chester disease. *Curr Rheumatol Rep*, 2014; 16 (4): 412
3. Mazor RD, Manevich-Mazor M, Shoenfeld Y: Erdheim-Chester disease: A comprehensive review of the literature. *Orphanet J Rare Dis*, 2013; 8: 137
4. Cavalli G, Guglielmi B, Berti A et al: The multifaceted clinical presentations and manifestations of Erdheim-Chester disease: comprehensive review of the literature and of 10 new cases. *Ann Rheum Dis*, 2013; 72(10): 1691–95
5. Diamond EL, Dagna L, Hyman DM et al: Consensus guidelines for the diagnosis and clinical management of Erdheim-Chester disease. *Blood*, 2014; 124(4): 483–92
6. Cives M, Simone V, Rizzo FM et al: Erdheim-Chester disease: A systematic review. *Crit Rev Oncol Hematol*, 2015; 95: 1–11
7. Dickson BC, Pethe V, Chung CT et al: Systemic Erdheim-Chester disease. *Virchows Arch*, 2008; 452: 221–27
8. Allen TC, Chevez-Barrios P, Shetlar DJ et al: Pulmonary and ophthalmic involvement with Erdheim-Chester disease: A case report and review of the literature. *Arch Pathol Lab Med*, 2004; 128: 1428–31
9. Kenn W, Eck M, Alolio B et al: Erdheim-Chester disease: Evidence for a disease entity different from Langerhans cell histiocytosis? Three cases with detailed radiological and immunohistochemical analysis. *Hum Pathol*, 2000; 31: 734–39
10. Haroche J, Arnaud L, Cohen-Aubart F et al: Erdheim-Chester disease. *Rheum Dis Clin North Am*, 2013; 39(2): 299–311
11. Antunes C1, Graça B, Donato P: Thoracic, abdominal and musculoskeletal involvement in Erdheim-Chester disease: CT, MR and PET imaging findings. *Insights Imaging*, 2014; 5: 473–82
12. Haroche J, Cluzel P, Toledano D et al: Images in cardiovascular medicine. Cardiac involvement in Erdheim-Chester disease: Magnetic resonance and computed tomographic scan imaging in a monocentric series of 37 patients. *Circulation*, 2009; 119: e597–98
13. Gupta A, Kelly B, McGuigan JE: Erdheim-Chester disease with prominent pericardial involvement: clinical, radiologic, and histologic findings. *Am J Med Sci*, 2002; 324: 96–100
14. Egan A, Sorajja D, Jaroszewski D et al: Erdheim-Chester disease: The role of video-assisted thoracoscopic surgery in diagnosing and treating cardiac involvement. *Int J Surg Case Rep*, 2012; 3: 107–10
15. Yuceler Z, Kantarci M, Karabulut N et al: Multidetector computed tomographic imaging of Erdheim-Chester disease. *Tex Heart Inst J*, 2014; 41: 338–40
16. Raptis DA, Raptis CA, Jakerst C et al: Erdheim-Chester disease with interatrial septum involvement. *J Thorac Imaging*, 2011; 27: W105–7
17. Alharthi MS, Calleja A, Panse P et al: Multimodality imaging showing complete cardiovascular involvement by Erdheim-Chester disease. *Eur J Echocardiogr*, 2010; 11: E25
18. Egan AJ, Boardman LA, Tazelaar HD et al: Erdheim-Chester disease: clinical, radiologic, and histopathologic findings in five patients with interstitial lung disease. *Am J Surg Pathol*, 1999; 23: 17–26
19. Wittenberg KH, Swensen SJ, Myers JL: Pulmonary involvement with Erdheim-Chester disease: Radiographic and CT findings. *Am J Roentgenol*, 2000; 174: 1327–31
20. Arnaud L, Pierre I, Beigelman-Aubry C et al: Pulmonary involvement in Erdheim-Chester disease: A single-center study of thirty-four patients and a review of the literature. *Arthritis Rheum*, 2010; 62(11): 3504–12
21. Drier A, Haroche J, Savatovsky J et al: Cerebral, facial, and orbital involvement in Erdheim-Chester disease: CT and MR imaging findings. *Radiology*, 2010; 255(2): 586–94
22. Arnaud L, Hervier B, Neel A et al: CNS involvement and treatment with interferon- α are independent prognostic factors in Erdheim-Chester disease: A multicenter survival analysis of 53 patients. 2011; 117(10): 2778–82
23. Wilejto M, Abla O: Langerhans cell histiocytosis and Erdheim-Chester disease. *Curr Opin Rheumatol*, 2012; 24(1): 90–96
24. Karcioğlu ZA, Sharara N, Boles TL, Nasr AM: Orbital xanthogranuloma: Clinical and morphologic features in eight patients. *Ophthalm Plast Reconstr Surg*, 2003; 19(5): 372–81
25. Veyssier-Belot C, Cacoub P, Caparros-Lefebvre D et al: Erdheim-Chester disease. Clinical and radiologic characteristics of 59 cases. *Medicine (Baltimore)*, 1996; 75: 157–69
26. Gotthardt M, Welcke U, Brandt D et al: The role of bone scintigraphy in patients with Erdheim-Chester disease. *Clin Nucl Med*, 2000; 25: 414–20
27. Perlat A, Decaux O, Sébillot M et al: Erdheim-Chester disease with predominant mesenteric localization: Lack of efficacy of interferon alpha. *Joint Bone Spine*, 2009; 76: 315–17
28. Haroche J, Amoura Z, Trad SG et al: Variability in the efficacy of interferon-alpha in Erdheim-Chester disease by patient and site of involvement: Results in eight patients. *Arthritis Rheum*, 2006; 54: 3330–36
29. Houston BA, Elliott Miller PE, Rooper LM et al: From dancing to debilitated. *N Engl J Med*, 2016; 374: 470–77